Neat fuel influence on biodiesel blend emissions

G J Thompson* and **J Nuszkowski**
Department of Mechanical and Aerospace Engineering, West Virginia University, Morgantown, West Virginia, USA

The manuscript was accepted after revision for publication on 18 August 2009.

DOI: 10.1243/14680874JER04909

Abstract: The emissions of oxides of nitrogen (NO_x) from biodiesel blended fuels reported in the literature vary from an NO_x increase to an NO_x decrease relative to the neat petroleum diesel fuel (PDF). To explain these NO_x differences, three PDFs with varying fuel properties were admixed with a neat soy-derived biodiesel at 10 per cent and 20 per cent volume ratios and evaluated using a heavy-duty diesel engine exercised over transient and steady-state cycles. The PDFs with 'low' and 'medium' cetane numbers led to a change in combustion phasing when blended with the neat biodiesel, resulting in reduced NO_x emissions at low engine power. The B100 blended with the 'high'-cetane-number PDF showed minimal change in combustion phasing and resulted in an NO_x increase at all engine loads. The derived peak in-cylinder gas temperature variation correlated with the brake-specific NO_x emissions indicating that the thermal NO_x formation responds to the addition of biodiesel. The biodiesel blends had an NO_x–particulate matter trade-off, also suggesting a thermal NO_x effect. The increase in NO_x emissions of the biodiesel blends also had a strong correlation with the level of saturated hydrocarbons at high engine power.

Keywords: heavy-duty, diesel, biodiesel, oxides of nitrogen, combustion, emissions, heat release

1 INTRODUCTION

Diesel engines are widely used power plants owing to their durability and high fuel efficiency compared with other types of internal combustion engine. With no reliable, cost-effective, alternative method of power production with the same advantages, diesel engines will continue to be used in the near future for commercial and industrial applications. Pollutants are a major issue from diesel engines, with oxides of nitrogen (NO_x) and airborne particulate matter (PM) receiving particular attention. These and other pollutants in diesel exhaust have been identified to cause adverse health effects [**1**, **2**]. To reduce air pollution, the US Environmental Protection Agency and other regulatory agencies worldwide have tightened diesel engine emissions standards over the last two decades [**3**].

One aspect of diesel research has focused on biodiesel, which is derived from vegetable oil or tallow (animal fat), as a means of reducing emissions from the existing, or legacy, fleet. Biodiesel, being a renewable energy source, benefits in the reduction of life-cycle CO_2 emissions. Additionally, naturally available biofuels are seen as one means of reducing imported petroleum. Some main engine emissions advantages of biodiesel are the higher cetane rating, no (or very low) aromatics, and low or no sulphur content [**4**]. From an atmospheric perspective, biodiesel benefits with respect to climate change gases have been addressed in the GREET model [**5**]. Although suffering from having lower energy content and higher NO_x emissions (up to 13 per cent) compared with the neat petroleum diesel fuel (PDF), the emissions of total hydrocarbons (THC), CO, and PM have been shown to decrease by 13.6–63.2 per cent, 10.1–42.7 per cent, and 8.3–55.0 per cent, respectively [**4**, **6**], depending on blending ratio, fuel type, and test cycle. Some studies have offset the increase in NO_x emissions of biodiesel blends by the addition of a cetane improver [**7**–**9**] or

*Corresponding author: Department of Mechanical and Aerospace Engineering, West Virginia University, 349 Engineering Science Building, Morgantown, WV 26506, USA.
email: Gregory.Thompson@mail.wvu.edu

by lowering the iodine number (degree of unsaturation) [**7**]. For a Cummins ISB (2002 and 2003) engine using B20 (20 per cent by volume neat biodiesel and 80 per cent neat petroleum diesel) fuel, McCormick [**10**] saw an average 25 per cent decrease in PM and 3 per cent increase in NO_x compared with the neat PDF. The addition of a cetane improver showed no effect in comparison to previous research done on older engine technology by McCormick *et al.* [**8**, **9**].

A recent study by Cheng and colleagues [**11**] investigated the NO_x emissions of biodiesel using optical techniques. The study suggests that the decrease in soot lowers radiation heat transfer, which causes increased local flame temperatures. Another suggested cause of increased NO_x was the different combustion chemistry and mixture stoichiometry relative to petroleum diesel. Using simulations and experiments on a 2004–2006 5.9 L ISB Cummins engine with cooled exhaust gas recirculation (EGR), Eckerle and co-workers [**12**] separated changes in NO_x due to using B20 fuel into engine calibration changes (−4.5 to 3.5 per cent) and combustion effects (1 to 5 per cent). The most significant engine calibration differences attributed to changes in NO_x were the EGR (intake oxygen) and start of injection (SOI). Szybist *et al.* [**13**] showed that the higher bulk modulus (compressibility) of biodiesel increased the SOI by 0.1–0.3 crank-angle degrees resulting in a phase shift of the maximum cylinder temperature and maximum heat release. Nuszkowski *et al.* [**14**] showed no significant difference between the neat fuel and the B20 biodiesel blends' heat release curves at high load while having up to 14 per cent increase in NO_x.

Biodiesel may be considered an oxygenate additive, which raises the local air-to-fuel ratio, thus resulting in increased oxygen at locations of fuel burning and providing a greater opportunity for soot oxidation. Previous studies [**15**–**17**] have shown a greater than 4 per cent reduction of PM for each 1 per cent (by weight) oxygen addition to the fuel. With an increase in oxygen content using a biodiesel compound (rapeseed methyl ester) or glycol ethers, Zannis *et al.* [**18**] reported a decrease in soot, CO, and THC emissions with an increase in NO_x emissions and brake-specific fuel consumption (FC) on a single-cylinder engine operating at 2000 r/min and three different loads. Using a blend of dimethyl carbonate with diesel at an oxygen content of 15 per cent, Lu and colleagues [**19**] found that smoke decreased by 75 per cent and NO_x emissions decreased by 15–20 per cent. The chemical structure of the oxygenate addition seems to affect the soot reduction, with glycol ethers showing greater reduction of soot than dioxolane [**20**]. It should be noted that studies concerning relative emissions of blended and/or additized diesel utilized different petroleum diesel as a baseline and the variability of the baseline petroleum diesel may be the cause of varying results. With typical pump diesel fuels commercially available in the USA, Thompson and co-workers [**21**] showed a variation of 12 per cent in the NO_x, 46 per cent in the PM, 11 per cent in the CO, and 30 per cent in the THC emissions for the same engine and test cycle.

Fuels with different ignition characteristics will have different start of combustion locations resulting in changes in the combustion phasing; the authors refer to this as a 'cetane effect' throughout the current paper. While the actual ignition delay may be more of a significant factor affecting emissions than the measured cetane number, a fuel supplier or a researcher without the tools to measure heat release rate or injector needle lift will utilize the fuel properties as a tool to determine the desired fuel blending ratio.

A common trend in diesel engine research is the NO_x–PM trade-off. At higher combustion temperatures PM is oxidized, resulting in lower PM produced, but a high formation rate of NO_x occurs due to the Zeldovich mechanism. At low combustion temperatures, more PM forms due to incomplete combustion, but less NO_x is formed. The authors refer to this temperature trend as the 'combustion temperature effect'.

The effect of biodiesel on emissions continues to be studied; particularly NO_x and PM. The present paper focuses on the influence of the neat PDF on biodiesel blends' emissions in a heavy-duty diesel engine. Three neat fuels with different fuel properties (particularly cetane number and aromatic level) were studied with 10 (10 per cent by volume neat biodiesel and 90 per cent neat PDF) and 20 per cent soy-derived biodiesel blends; these blends are termed B10 and B20, respectively, in this paper. A 1992 Detroit Diesel Series 60 engine was chosen for this study since it was a production engine and representative of legacy engines while having robust electronic controls to provide for repeatable measurements. The use of a modern (circa 2009) diesel engine for combustion would involve increased emission control devices (injection rate shaping, higher injection pressure, EGR, and variable geometry turbocharger) and these additional controls may mask the subtle fuel-related combustion effects due to the variability in these additional control mechanisms. The electronic control unit settings were not

modified between fuels, so the results represent real-world conditions that may be expected from legacy engines. The combustion characteristics were analysed by use of an in-cylinder pressure transducer during steady-state and transient tests. Correlations between the fuel properties, in-cylinder pressure data, and emissions were studied.

2 HEAT RELEASE ANALYSIS

The approach used in this paper to extract heat release information involved the use of a traditional single-zone zero-dimensional heat release model [**22**]. While spatial characteristics internal to the cylinder are not studied, conclusions may still be drawn on the spatially averaged burn rate. The first law of thermodynamics was applied to a single-zone mixture in the cylinder of a diesel engine between the intake valve closing and the exhaust valve opening. The gross heat release, equation (1), provides the total heat released including the energy lost to the cylinder walls. The well-known Woschni model [**23**] for the heat transfer coefficient and the mean gas cylinder temperature were used to adjust the net heat release to yield an estimated true burn rate. Although the ratio of specific heats was assumed constant in the derivation of the heat release equation, the quantity varies with temperature and gas quantities. To account for these effects an iterative approach was used. The specific heat ratio given by Brunt and Platts [**24**] was used for the first iteration and then solving for the exhaust constituents (O_2, CO_2, H_2O, and N_2) assuming complete combustion. The exhaust constituents were solved from the heat release (converted to fuel mass) and intake air flow (from density of charge and displacement). Knowing the exhaust and intake ratio of specific heats, the cylinder average specific heat ratio during burning was solved using the mass fraction burned as the ratio of exhaust to total constituents, equation (2)

$$\left[\frac{\mathrm{d}Q}{\mathrm{d}\theta}\right]_{\text{Gross}} = \left(\frac{\gamma}{\gamma-1}\right)\cdot P\cdot\frac{\mathrm{d}V}{\mathrm{d}\theta} + \left(\frac{1}{\gamma-1}\right)\cdot V\cdot\left[\frac{\mathrm{d}P}{\mathrm{d}\theta}\right] + \left[\frac{\mathrm{d}Q}{\mathrm{d}\theta}\right]_{\text{Heat transfer}} \quad (1)$$

$$\gamma_{\text{Average}}(T, y_i) = [1 - mfb]\cdot\gamma_{\text{Intake}}(T, y_i) + mfb\cdot\gamma_{\text{Exhaust}}(T, y_i) \quad (2)$$

where

Q	heat energy
θ	crank angle
γ	ratio of specific heats
P	in-cylinder pressure
V	volume
T	temperature
y_i	concentration of species i
mfb	mass fraction burned

3 EXPERIMENTAL SETUP

A 1992 Detroit Diesel Series 60 engine was used to study the influence of the neat diesel fuel in biodiesel blends for an on-road heavy-duty diesel engine in the USA (Fig. 1). The engine was a turbocharged, intercooled, and electronically controlled (Table 1). The engine hardware and electronic control was deemed representative of the on-road legacy engines in the USA today that are the high emissions emitters of concern. There is a wide variety of feedstocks for biodiesel; these include rapeseed, soybean, sunflower, coconut oil, palm oil, beef tallow, chicken fat, fish oil, and others. The soy-derived biodiesel was chosen for the present study owing to wide use in the USA.

Fig. 1 WVU test cell with 1992 Detroit Diesel Series 60 engine mounted

Table 1 Engine specifications

Manufacturer	Detroit Diesel
Model number	Series 60
Model year	1992
Engine configuration	Inline 6
Displacement (l)	12.7
Power rating (kW)	268 at 1810 r/min
Torque rating (Nm)	1966 at 1200 r/min
Bore (mm) × stroke (mm)	130 × 160
Connecting rod length (mm)	269.3
Compression ratio	15:1
Intake	Turbocharged & intercooled

Three neat petroleum fuels with a range of cetane numbers were investigated. The fuel properties are included as Table 2. The neat PDFs were named Low Cetane (LC), Middle Cetane (MC), and High Cetane (HC) and their blends of neat biodiesel fuel at 10 per cent and 20 per cent levels were named B10 and B20, respectively. The neat biodiesel fuel was named B100. The cetane numbers of the LC, MC, and HC fuels were 42.4, 49.2, and 62.5, respectively. It should be noted that the MC fuel had a sulphur content of 341 ppmw. Although present US on-road diesel fuel is required to be ultra-low sulphur (below 15 ppmw), the MC fuel was a '500 ppmw' low-sulphur fuel. The high hydrogen content of the HC fuel provided a low density fuel (801.8 g/l) with a low initial boiling point of 167 °C; this fuel is close to a number 1 diesel in the USA. The total aromatics (ASTM D5186, by percentage mass) of the diesel fuels were 42.2 for the LC fuel, 34.2 for the MC fuel, and 9.1 for the HC fuel. The LC fuel was chosen because of the low cetane number, and had a longer ignition delay than the MC and HC fuels. The B100 fuel had a cetane number of 59.9, so the LC B10, LC B20, MC B10, and MC B20 blends had higher cetane numbers then their respective neat fuels while the HC B10 and HC B20 fuels' cetane numbers decreased relative to the HC fuel. The near zero aromatics of a B100 fuel should decrease the aromatics of the B10 and B20 blends, irrespective of the neat petroleum diesel aromatic levels. The total aromatics of the B10 and B20 blends shown in Table 2 were calculated assuming a linear distribution with B100 having zero aromatics. For the B100 fuel, the saturated hydrocarbons were assumed at 13 per cent (by volume) [**25**] and the olefins, the remaining 87 per cent. The B10 and B20 saturated hydrocarbons and olefins were then calculated assuming a linear distribution between the neat PDFs and B100. An attempt was made to measure the aromatic level of the B100, B10, and B20 blends utilizing the ASTM D1319 and D5186 test methods, but there was a hang-up of the biodiesel in the silica gel column and an interference issue was revealed due to similar retention times of the ester compounds in the biodiesel fuels and aromatics in the diesel fuels [**26**].

The full-scale dilution, constant-volume system employed in the test cell was designed based on Title 40 CFR Part 86 Subpart N requirements [**3**]. A critical flow venturi was used as the method of measuring the diluted exhaust. The dilute exhaust analysers consisted of a Rosemount Analytical model 402 heated flame-ionization detector, a Rosemount model 955 heated, wet chemiluminescent analyser, a Horiba model AIA–210LE non-dispersive infrared (NDIR) analyser, and a Horiba model AIA-210 NDIR analyser to measure THC, NO_x, CO, and CO_2, respectively. The PM was measured gravimetrically in accordance with Title 40 CFR Part 86 Subpart N requirements using proportional sampling of the diluted exhaust through a pair of Pallflex (70 mm diameter) model T60A20 fluorocarbon-coated glass microfibre filters in series using a secondary dilution tunnel.

An R&P 1105 tapered element oscillating microbalance (TEOM) was used to measure continuous PM. As a sample of diluted exhaust is pulled through a small filter, which is attached to an oscillating element, the resonant frequency of the oscillating element correlates with the PM build-up on the small filter. The inferred PM mass on the filter and the flow rate through the TEOM are related to obtain a PM mass concentration (mg/m^3). The engine-out PM flow can then be obtained through knowledge of the dilution tunnel flow. Utilizing a TEOM for PM has been shown to correlate with gravimetric filter measurements, although there is typically a 10–15 per cent offset between the two measurements [**27**, **28**]. The TEOM gives an indication of the total particulate matter (TPM) generation during a transient or steady-state test.

An engine test sequence consisted of a warm-start heavy-duty Federal Test Procedure (FTP) test followed by three hot-start FTP tests; only the hot-start FTP results are presented. The warm-start test was used to bring the engine to normal operating conditions. In between each test was a 20 min soak period used for zero and spanning the analysers, changing PM filters, and data collection.

After the last hot-start FTP data collection, the steady-state Supplemental Emissions Test (SET) was performed since this test is now required as part of the engine certification procedure for new on-road heavy-duty diesel engines in the USA. Additionally, the SET provides a link to prior biodiesel literature performed at steady state. The SET consists of an idle mode and four loads at three different engine speeds (12 modes) with the duration of idle lasting 4 min and the 12 other modes lasting 2 min (see Fig. 2). The numbers in Fig. 2 indicate the order in which the steady-state points were tested and are used as the mode numbers referenced in this paper. The engine speeds A, B, and C are determined from the engine power curve and represent low-, intermediate-, and high-speed operation, respectively. Typically, the SET emissions are reported as an averaged weighted value based on published weight-

Table 2 Fuel properties

Test method	Fuel property	Units	LC	LC B10 soy	LC B20 soy	MC	MC B10 soy	MC B20 soy	HC	HC B10 soy	HC B20 soy	B100
EN14078	FAME	vol%	0.0	10.6	21.0	0.0	10.1	20.9	0.0	9.8	20.8	N/A
D4052s	Density at 15 °C	g/l	864.0	866.2	868.2	848.1	851.7	855.6	801.8	809.7	818.0	885.2
D445 40c	Viscosity	mm^2/s	2.511	2.62	2.768	2.69	2.804	2.961	2.075	2.2	2.4	4.154
D613	Cetane no.	–	42.4	46.3	46.2	49.2	50.8	51.1	62.5	62.9	62.3	59.9
D5186	Total aromatics	mass%	42.2	38.0*	33.8*	34.2	30.8*	27.4*	9.1	8.2*	7.3	0.0
	Mono aromatics	mass%	31.6	28.4*	25.3*	24.8	22.3*	19.8*	7.7	6.9*	6.2*	0.0
	Poly aromatics	mass%	10.6	9.5*	8.5*	9.4	8.5*	7.5*	1.4	1.3*	1.1*	0.0
D1319	Aromatics	vol%	45.8	41.2*	36.6*	34.3	30.9*	27.4*	6.8	6.1*	5.4*	0.0
	Olefins	vol%	3.8	12.1*	20.4*	2.3	10.8*	19.2*	3.2	11.6*	20.0*	87.0†
	Saturates	vol%	50.4	46.7*	42.9*	63.4	58.4*	53.3*	90.0	82.3*	74.6*	13.0†
D4629	Nitrogen	ppm	42.6	33.7	32.5	70.6	63.3	39.9	1.4	1.4	1.4	1.2
D5453	Sulphur	ppm	6.7	4.3	4.4	340.7	298.4	254.1	3.2	1.6	1.9	1.4
D5291	Carbon	wt%	87.4	86.1	85.1	86.8	85.6	84.8	85.5	85.3	83.9	78.2
	Hydrogen	wt%	12.7	12.5	12.4	13.0	12.9	12.9	14.4	14.3	13.9	12.0
	Oxygen	wt%	0.00	0.98*	1.96*	0.00	0.98*	1.96*	0.00	0.98*	1.96*	9.78‡
	Total	wt%	100.0	99.6	99.5	99.8	99.4	99.6	99.9	100.5	99.7	100.0
	H-to-C	–	1.73	1.73	1.74	1.79	1.80	1.81	2.00	1.99	1.98	1.83
	O-to-C	–	0.000	0.009	0.017	0.000	0.009	0.017	0.000	0.009	0.018	0.094
D86	Initial boiling point	°C	190.2	186.7	191.8	179.4	180.0	195.7	166.6	166.1	166.5	284.4
	5%	°C	205.3	204.4	210.0	198.0	204.9	214.5	179.2	179.7	183.1	330.6
	10%	°C	216.6	218.5	222.9	212.6	218.9	229.5	185.9	186.8	188.6	333.7
	15%	°C	223.2	225.7	230.0	222.2	229.1	237.9	191.2	192.9	197.0	334.4
	20%	°C	227.7	231.8	236.8	230.8	236.4	244.2	197.3	199.7	205.2	334.7
	30%	°C	238.0	242.5	248.4	245.1	250.7	256.3	208.8	213.6	222.7	335.3
	40%	°C	247.7	252.7	260.6	256.4	262.6	267.0	222.9	230.7	244.8	336.0
	50%	°C	256.3	263.2	273.2	265.9	274.2	277.7	238.3	250.3	267.9	336.4
	60%	°C	265.5	274.6	287.4	275.4	285.8	290.5	256.1	271.4	290.6	337.4
	70%	°C	275.9	287.8	302.1	286.7	299.0	304.5	274.1	291.9	308.7	338.2
	80%	°C	288.5	303.3	317.3	300.9	314.3	318.8	293.6	309.3	320.9	340.2
	90%	°C	306.6	321.4	330.7	320.0	329.2	331.3	311.1	323.2	330.1	345.7
	95%	°C	321.2	331.6	337.5	333.7	339.8	338.4	320.4	329.7	334.9	344.0
	Final boiling point	°C	335.2	340.4	346.3	346.8	350.4	347.9	328.7	336.9	341.2	345.2
	Recovered	ml	97.8	97.7	98.5	98.6	99	98.3	98.4	98.1	97.9	96.6
	Residue	ml	1.0	1.2	0.6	0.5	0.7	0.5	0.5	0.9	1.2	1.6
	Loss	ml	1.2	1.1	0.9	0.9	0.3	1.2	1.1	1.0	0.9	1.8
D93	Flash point	°C	73.9	77.2	76.7	70.6	74.4	82.8	59.4	60.0	60.6	148.3
WVU	LHV	MJ/kg	42.34	41.76	41.28	42.54	41.95	41.50	43.35	42.65	41.99	37.15

N/A, not available.
*Linear interpolation between the base fuel and B100.
†Assumed based on reference [**24**].
‡Solved assuming oxygen accounted for the rest of the weight.

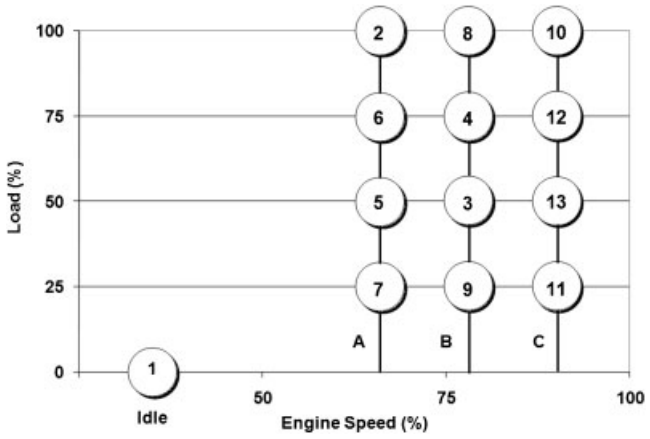

Fig. 2 SET steady-state locations

ing factors for each mode. For this study, the mass emissions during each mode were more important and were addressed separately. It should be noted that use of the idle mode has been excluded from the data analysis because this mode's data are at the lower end of many systems' resolution since the sampling system was configured to obtain the best response at the high power modes.

In-cylinder pressure was acquired using a Kistler model 6125B transducer with a model 5010B charge amplifier. The in-cylinder pressure was acquired from one cylinder at 0.25 degree crank-angle resolution. A low-pass filter with a cut-off frequency of 2500 Hz was applied to the in-cylinder pressure to reduce the high-frequency combustion noise. The dynamic pressure of the in-cylinder pressure transducer was referenced using a constant polytropic coefficient. For steady-state testing, 200 consecutive pressure curves were averaged at the end of each sampling period. For the transient testing, an average of the three hot-start FTP tests was used to determine the average heat release information. The combustion characteristics (gross indicated mean effective pressure, mean cylinder gas temperature, etc.) were solved using methods from previous researchers [**24**, **29**, **30**]. The SOI was acquired from a needle lift sensor inside the fuel injector for cylinder 3. The definition of start of combustion used by the authors was the local minimum in the heat release curve before the premix spike, thought to occur from the fuel evaporating. The mean cylinder gas temperature was calculated from the ideal gas law ($T = PV/mR$, where T, P, and V have their previous meanings; m is mass and R is the ideal gas constant) using the in-cylinder pressure, cylinder volume, and the intake valve closing (IVC) as a reference condition ($T = PV(T_{IVC}/P_{IVC}V_{IVC})$). The cylinder gas temperature at intake valve closing was assumed to be equal to the intake manifold temperature, which was measured from a thermocouple in the intake manifold.

4 EMISSION RESULTS

The integrated brake-specific results of FC, THC, CO, NO_x, and PM from the FTP testing are presented in Table 3. Student's t test was performed comparing the biodiesel blends with their respective neat PDFs. The percentage reductions are shown only for statistically significant values with a P value of < 0.05. Up to a 2.9 per cent increase in brake-specific FC with the biodiesel blends was seen compared with the neat PDFs. The increase in FC may be due to the oxygen content (and hence lower energy content) in biodiesel. The B10 and B20 blends in this study had 1.0 per cent and 2.0 per cent oxygen content, respectively (Table 2). A significant reduction in brake-specific THC (up to 18 per cent), CO (up to 12 per cent), and TPM (up to 20 per cent) was seen for the B10 and B20 blends compared with the neat PDFs. Previous studies have seen similar reductions in these constituents [**4**, **6**, **8**] when using biodiesel, although the effect on NO_x varied. During

Table 3 Average hot-start integrated brake-specific FTP results and percentage differences with respect to the neat PDF

		Brake-specific FC		CO		NO_x		THC		TPM	
Blend	Base	g/kWh	Diff (%)	g/kWh	Diff (%)	g/kWh	Diff (%)	g/kWh	Diff (%)	g/kWh	Diff (%)
–	LC	225	–	4.97	–	7.22	–	0.140	–	0.347	–
B10	LC	229	1.6	4.65	−6.4	7.23	*	0.125	−10.5	0.314	−9.6
B20	LC	232	2.9	4.37	−12.1	7.21	*	0.114	−18.2	0.276	−20.4
–	MC	227	–	4.70	–	6.88	–	0.123	–	0.352	–
B10	MC	229	1.0	4.40	−6.4	6.86	*	0.115	−6.4	0.318	−9.8
B20	MC	231	1.9	4.17	−11.4	6.90	*	0.107	−13.3	0.280	−20.3
–	HC	224	–	3.77	–	5.86	–	0.117	–	0.299	–
B10	HC	227	1.5	3.60	−4.6	6.03	2.8	0.115	*	0.269	−10.3
B20	HC	231	2.9	3.50	−7.3	6.17	5.2	0.105	−10.1	0.243	−18.9

*No significant difference using a t test with $P < 0.05$.

the FTP tests in this study, either a significant increase in NO_x was seen (2.8–5.2 per cent for the HC fuel B10 and B20 blends) or no significant difference was seen, as was the case with the LC and MC B10 and B20 blends. It should be noted that the NO_x FTP emissions were significantly different between the PDFs. There was a 23.2 per cent difference between the HC and LC PDFs' NO_x emissions, which was four times greater than any NO_x differences noticed between blending biodiesel with a given PDF.

The NO_x response for the B10 and B20 blends were dependent on load, neat PDF, and blend concentration. A sixth-order polynomial was fit to the continuous NO_x mass rate as a function of power from the FTP test for all fuels. Using these sixth-order polynomials, the percentage change in NO_x as a function of power was calculated for the B10 and B20 blends (Fig. 3). The reduction of the maximum power with decreasing density (increasing cetane number) for the neat PDFs was noticeable. As load increased for the LC and MC B10 and B20 blends, NO_x changed from an NO_x reduction to an NO_x increase between 119 and 160 kW. The HC B10 and B20 fuels showed a 1.0–3.9 per cent and 2.0–6.1 per cent increase, respectively, of power range over the HC fuel. Therefore, an engine operating at low load, such as in an urban environment, would have an NO_x benefit with LC and MC B10 and B20 blends. Contrarily, a HC B10 or B20 blend, or a heavy-duty diesel engine operating at high load, would have an adverse effect on NO_x. This explains why some of the literature for transient engine testing (engine or chassis dynamometer) may or may not show the NO_x 'bump'. A transient test cycle with a relatively low duty cycle, such as the FTP at ~25 per cent average rated power, exhibits an NO_x reduction using a B20 blend made from neat petroleum with a 'low' cetane number and neat biodiesel with a 'high' cetane number. Likewise, an NO_x increase is seen when the cetane numbers of the two fuels are closely matched.

For the steady-state testing, only one test per fuel was used owing to time and fuel constraints. Therefore a statistical analysis was not performed. The steady-state testing was undertaken to understand the difference between low and high load conditions that created the varied NO_x characteristics for the different neat fuels used on the biodiesel blends with the engine exercised over the FTP cycle. Figures 4(a) and (b) depict the percentage change of the modal brake-specific emissions of NO_x for the biodiesel blends compared with their respective neat fuel at low load (25 per cent load) and high load (100 per cent load), respectively, during the steady-state testing. For 25 and 100 per cent load, there were

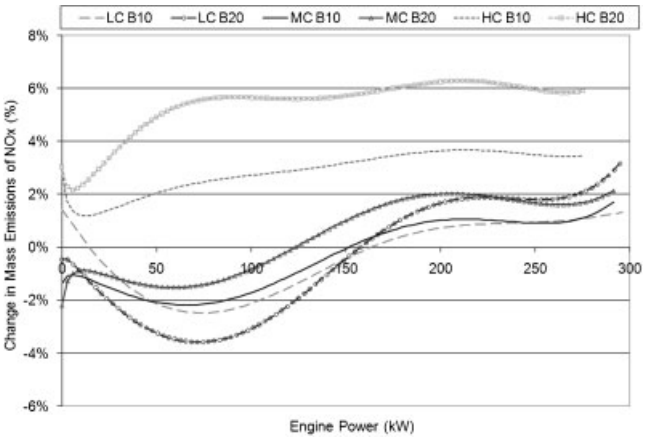

Fig. 3 Percentage change of NO_x for the biodiesel blends with respect to their neat fuel from the polynomial curve fit of NO_x as a function of power for each fuel

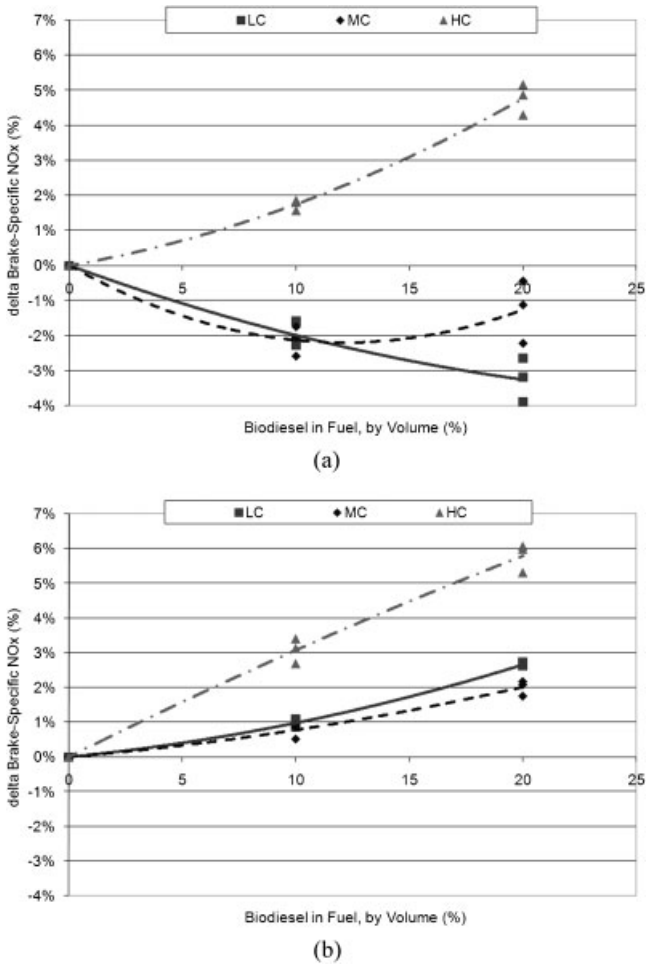

Fig. 4 Steady-state brake-specific NO_x from SET testing: (a) 25% load; (b) 100% load

three modes, each at three different engine speeds. At 100 per cent load (Fig. 4(b)), an almost linear increase in NO_x with an increase in the volume percentage of biodiesel occurred. The HC B10 and B20 blends had the largest increase in NO_x whereas the LC and MC B10 and B20 blends had a much lower rate and were within 1 per cent of each other. At 25 per cent load (Fig. 4(a)), a different trend was noticed for the LC and MC B10 and B20 fuels compared with the HC B10 and B20 fuels. The HC B10 and B20 fuels exhibited an NO_x increase of 1.5 per cent and 5 per cent, respectively, while the LC B10 and B20 fuels showed approximately a linear NO_x decrease with increasing biodiesel concentration. The MC B10 was virtually identical to the LC B10, but the MC B20 fuel showed only ~ 1 per cent decrease in NO_x compared with ~ 3 per cent decrease with LC B20. These results mimic the results found in Fig. 3. It is speculated that the MC and LC fuels admixed with higher concentrations of B100 (i.e. B30, B50, etc.) would show an NO_x increase at low load. Zhang and Boehman [**31**] found similar results to the LC and MC fuels with a slight reduction in NO_x at low load and an increase in NO_x at high load when blending biodiesel and diesel.

5 COMBUSTION CHARACTERISTICS

In-cylinder pressure was collected for the steady-state and transient tests. The fuel flow derived from combustion was compared with the laboratory fuel meter and emissions-derived fuel flow for all steady-state modes and fuels tested. The cumulative heat release in the cylinder with pressure measurement was assumed to be the same for all six cylinders and was then converted to fuel flow using the energy content of the fuel and the engine speed, equation (3). A linear regression constrained to pass through the origin showed good agreement, with a slope of 0.97–0.99 and an R^2 of 0.991–0.998. This comparison was used as a quality check for the heat release computation

$$m_{\text{fuel}} = \frac{Q_{\text{cumulative}}}{LHV} \cdot n_{\text{s}} \cdot \frac{1}{2} \frac{cycle}{rev} \tag{3}$$

where

LHV	lower heating value
n_{s}	engine speed

The start of combustion, peak of the average in-cylinder gas temperature, the premix fraction, brake-specific NO_x, and brake-specific PM are provided for each steady-state mode in Table 4. For low loads (modes 7, 9, and 11), the B10 and B20 blends had an earlier start of combustion and lower premix fraction of total burn than their respective neat PDF (Fig. 5(a), mode 7). The HC B10 and B20 fuels had the lowest change in the heat release curve compared with the neat PDF. The LC and MC B10 and B20 fuels created an earlier start of combustion due to the higher cetane number of the B100, which resulted in a phase shift of the heat release curve. The early start of combustion decreased the amount of fuel available to burn during the premixed portion of the heat release curve. During the low load modes, the NO_x decreased for the LC and MC B10 and B20 fuels, suggesting a cetane effect as defined above. With B100 blended into petroleum diesel, the actual SOI will be affected by the bulk modulus of compressibility for the fuel [**11**, **13**]. Although this effect is more pronounced for pump-line-nozzle fuel injection, the 1992 DDC engine used in this study had unit injectors. It should be noted that SOI was directly measured and a 0.25 degree or less shift (0.25 degrees was the resolution of the encoder) was observed between neat PDF and B10 and B20 fuels.

For high loads (Fig. 5(b), mode 8), the heat release curves showed less of a change between the B10 and B20 fuels and their respective neat PDF than during low load. The location of 90 per cent mass fraction burned occurred at 30–33 degrees after top dead centre (ATDC) for all nine fuels. All B10 and B20 fuels showed an NO_x increase compared with their neat PDF at high load; the HC B10 and B20 fuels exhibited the greatest NO_x increase. In-cylinder pressure data were not available for the MC B10 fuel during steady-state testing, but in-cylinder pressure was collected during transient testing and the MC B10 fuel's heat release was found to behave between the MC and MC B20 fuels' heat release parameters.

Figure 6 shows a contour plot for the average premix fraction derived from the three hot-start FTP tests on the LC fuel. The maximum torque at each engine speed and the steady-state locations (from the SET test) on the engine map are also shown for reference. At high loads, the premix fraction was less than 0.1 and at low loads, the premix fraction was greater than 0.5. The premix fraction is a function of the ignition delay, which is a function of the cetane number [**32**–**34**]. Figure 7 displays the correlation of brake engine power and the ignition delay for the SET data. The increase in the cetane number of each LC and MC fuel was noticeable by the decrease in the y-intercept at relatively the same slope. The

Table 4 Steady-state emissions, peak in-cylinder temperature, start of combustion, and premixed burn fraction

		Start of combustion (degrees ATDC)			Peak in-cylinder temperature (K)			Premix fraction			NO_x (g/kWh)			PM – TEOM (g/kWh)		
Fuel	Mode	Neat	B10	B20	Neat	B10	B20	Neat	B10	B20	Neat	B10	B20	Neat	B10	B20
LC	1	—	—	0.5	1164	1095	1083	0.01	0.01	0.70	—	—	—	—	—	—
	2	−6.0	−6.3	−6.5	1855	1864	1869	0.07	0.07	0.06	8.12	8.20	8.34	0.35	0.32	0.28
	3	−4.0	−4.3	−4.5	1670	1679	1680	0.29	0.27	0.26	12.61	12.63	12.70	0.03	0.03	0.01
	4	−5.8	−6.0	−6.0	1727	1729	1734	0.14	0.14	0.13	10.24	10.33	10.46	0.08	0.07	0.06
	5	−3.5	−4.0	−4.3	1742	1743	1748	0.25	0.24	0.23	12.13	12.15	12.31	0.03	0.03	0.03
	6	−5.0	−5.3	−5.5	1806	1811	1819	0.13	0.12	0.11	9.49	9.54	9.71	0.14	0.12	0.10
	7	−1.8	−2.0	−2.5	1546	1542	1539	0.60	0.57	0.56	17.11	16.72	16.56	0.04	0.06	0.07
	8	−7.0	−7.0	−7.3	1781	1785	1781	0.08	0.08	0.08	9.25	9.33	9.50	0.14	0.12	0.11
	9	−2.3	−2.5	−2.8	1512	1509	1500	0.63	0.62	0.61	17.11	16.84	16.65	−0.01	0.06	0.00
	10	−7.5	−8.0	−8.0	1721	1724	1722	0.10	0.09	0.09	9.59	9.70	9.85	0.10	0.09	0.08
	11	−2.5	−2.8	−3.3	1484	1482	1483	0.66	0.64	0.62	17.37	17.01	16.70	0.04	0.05	0.03
	12	−6.3	−6.5	−6.8	1668	1679	1678	0.17	0.16	0.16	10.59	10.62	10.78	0.06	0.05	0.05
	13	−4.8	−5.0	−5.3	1626	1626	1637	0.32	0.31	0.30	12.84	12.77	12.96	0.03	0.03	0.03
MC	1	—	−0.3	−0.3	1143	1046	1002	0.01	0.67	0.65	—	—	—	—	—	—
	2	−6.3	N/A	−6.5	1853	N/A	1870	0.06	N/A	0.06	8.00	8.04	8.16	0.37	0.32	0.29
	3	−4.8	N/A	−5.0	1674	N/A	1669	0.25	N/A	0.23	12.16	12.16	12.30	0.01	0.01	0.01
	4	−6.3	N/A	−6.5	1734	N/A	1738	0.13	N/A	0.12	10.04	10.10	10.24	0.09	0.07	0.06
	5	−4.3	N/A	−4.5	1735	N/A	1742	0.21	N/A	0.20	11.68	11.66	11.87	0.03	0.04	0.03
	6	−5.5	N/A	−5.8	1814	N/A	1825	0.11	N/A	0.10	9.26	9.30	9.47	0.15	0.12	0.11
	7	−2.8	N/A	−3.0	1530	N/A	1526	0.53	N/A	0.50	15.46	15.19	15.40	0.05	0.08	0.07
	8	−7.3	N/A	−7.5	1774	N/A	1778	0.07	N/A	0.07	9.11	9.19	9.31	0.15	0.13	0.11
	9	−3.0	N/A	−3.5	1494	N/A	1484	0.56	N/A	0.55	15.55	15.23	15.37	0.02	0.02	0.04
	10	−7.8	N/A	−8.3	1720	N/A	1731	0.09	N/A	0.09	9.50	9.59	9.67	0.12	0.10	0.09
	11	−3.0	N/A	−3.8	1121	N/A	1466	0.96	N/A	0.57	15.80	15.39	15.45	0.02	0.06	0.08
	12	N/A	N/A	−7.0	N/A	N/A	1685	N/A	N/A	0.14	10.37	10.42	10.58	0.07	0.06	0.07
	13	N/A	N/A	−5.8	N/A	N/A	1626	N/A	N/A	0.27	12.31	12.16	12.37	0.03	0.04	0.05
HC	1	—	−2.3	—	1139	1033	1082	0.00	0.62	0.02	—	—	—	—	—	—
	2	−6.5	−6.8	−6.8	1838	1852	1853	0.05	0.05	0.05	7.35	7.55	7.74	0.35	0.31	0.27
	3	−5.5	−5.5	−5.5	1636	1642	1651	0.19	0.19	0.19	10.65	10.96	11.22	0.02	0.03	0.02
	4	−6.5	−6.8	−6.8	1710	1714	1722	0.11	0.10	0.10	9.10	9.34	9.60	0.08	0.07	0.06
	5	−4.8	−5.0	−5.0	1704	1712	1720	0.17	0.16	0.17	10.51	10.78	11.05	0.04	0.04	0.03
	6	−5.8	−6.0	−6.0	1785	1796	1803	0.09	0.08	0.08	8.56	8.79	9.02	0.14	0.11	0.10
	7	−3.8	−3.8	−3.8	1469	1473	1477	0.40	0.39	0.41	12.59	12.83	13.24	0.06	0.06	0.05
	8	−7.3	−7.5	−7.5	1765	1767	1770	0.06	0.06	0.06	8.19	8.44	8.68	0.15	0.13	0.11
	9	−4.3	−4.3	−4.3	1441	1439	1444	0.43	0.43	0.44	12.45	12.68	13.06	0.04	0.03	0.04
	10	−7.8	−8.0	−8.0	1708	1708	1718	0.08	0.08	0.08	8.58	8.88	9.10	0.10	0.08	0.07
	11	−4.5	−4.8	−4.8	1407	1413	1413	0.48	0.47	0.48	12.64	12.84	13.18	0.08	0.05	0.05
	12	−7.0	−7.3	−7.3	1664	1669	1672	0.13	0.12	0.12	9.31	9.58	9.88	0.10	0.05	0.04
	13	−6.0	−6.0	−6.0	1586	1580	1594	0.22	0.22	0.23	10.68	10.98	11.33	0.02	0.03	0.02

N/A, not available.
— indicates idle mode, no brake-specific work occurred at idle and/or no combustion occurred.

increased cetane number decreased the ignition delay. The HC fuel and the HC B10 and B20 fuels show similar trends without a decrease in ignition delay across all engine powers; the LC and MC B10 and B20 fuels did not exhibit this trend. Locations with a high premix fraction for the neat fuel are influenced by differences in the cetane number between the B10 and B20 fuels and the neat PDF. Figure 8 shows the correlation between the change in brake-specific NO_x and the change in premix fraction for the B10 and B20 fuels compared with the neat PDF from the SET. The LC B10 and B20 fuels had the highest correlations with an R^2 of 0.74–0.77 and the largest change in the premix fractions. The HC B10 and B20 fuels had the smallest change in premix fraction. When determining the change in NO_x emissions, the change in premix fraction between the neat PDF and the B100 fuel should be minimized when blending biodiesel into neat petroleum diesel to limit the influence of the heat release phase shift on the NO_x emissions as was done by Cheng and colleagues [**11**].

6 NO_X FORMATION

When studying combustion by means of the heat release, theories of NO_x formation have been suggested. The formation of NO_x is a function of temperature [**22**]. The temperature in combustion varies spatially and, therefore, the formation is linked to the local temperature. A major contribution to the understanding of NO_x formation was the study of Dec [**35**, **36**]. These studies showed that NO_x was

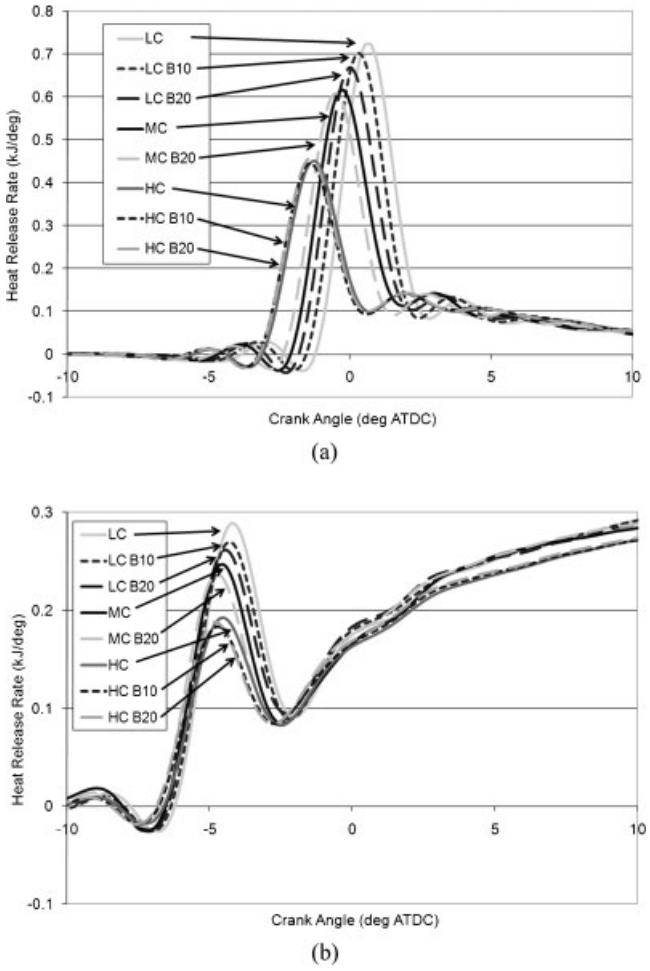

Fig. 5 Steady-state heat release rate: (a) mode 7, 25% load; (b) mode 8, 100% load

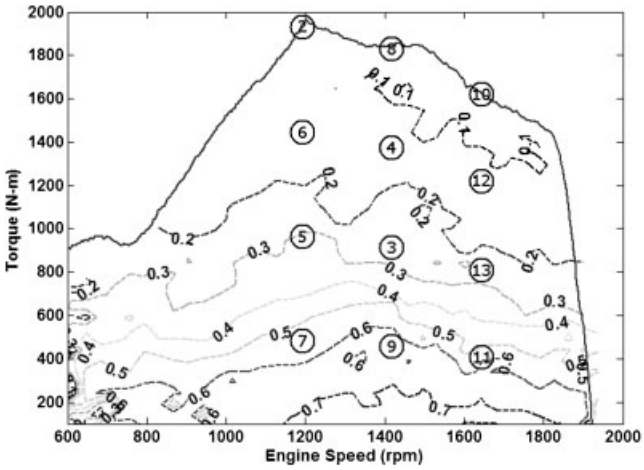

Fig. 6 FTP premix fraction for the MC fuel with the engine map and SET mode numbers

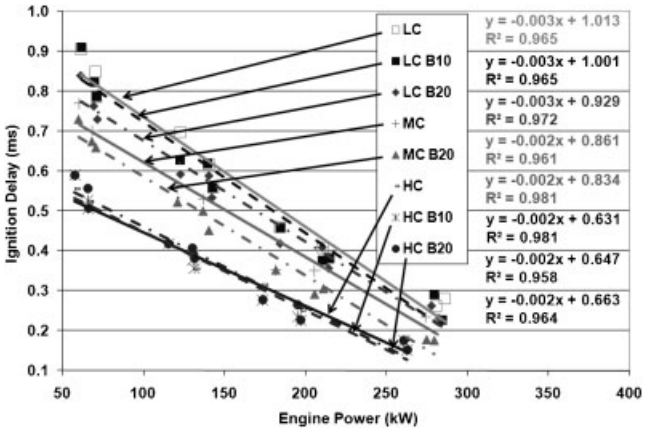

Fig. 7 Ignition delay for each fuel correlated with engine brake power

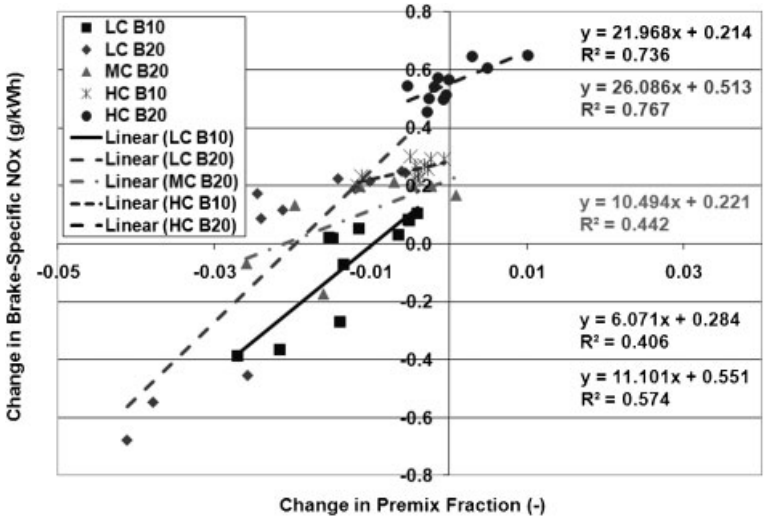

Fig. 8 Correlation of the change in the exhaust NO_x to the change in the premix fraction for the biodiesel blends with respect to their neat fuel from the steady-state modes

formed during the diffusion portion of the heat release, which is stoichiometric to lean, and not during the premix portion, which is rich. Dec [**35**, **36**] studied medium to high load conditions and not low load, where combustion is primarily premix combustion. There are many explanations for the change in NO_x emissions based on the heat release curve from previous researchers. Some accepted explanations for changes in NO_x are as follows.

1. An increase in the heat released during the premix portion corresponds to a rapid increase in the cylinder pressure and temperature compressing the diffusion flame where NO_x is formed; resulting in higher NO_x [**35**, **36**].
2. A decrease in the heat released during the premix portion of the heat release creates an increased amount of burning during the diffusion flame (mixing-controlled portion of the heat release) where NO_x is produced; resulting in higher NO_x [**33**, **35**, **36**].
3. A shift in the heat release towards top dead centre has higher pressure during combustion, which causes higher temperatures that lead to higher NO_x formation rates [**35**, **36**].
4. A long ignition delay leads to a uniform lean equivalence ratio due to better mixing. This typically occurs with high EGR (> 30 per cent). The combustion will then be closer to homogeneous charge compression ignition, which decreases NO_x due to lean combustion [**12**, **37**].

At low load, the LC and MC B10 and B20 fuels resulted in a decreased premix fraction, which would result in a less rapid increase in the cylinder pressure and temperature; resulting in decreased NO_x. For the current study, the NO_x increases were seen during high loads for the LC and MC B10 and B20 fuels and at all loads for the HC B10 and B20 fuels. The explanations for the NO_x increase cannot be derived from the heat release rate, but the peak of the spatially averaged in-cylinder gas temperature changes indicates that temperature was the driving force behind the brake-specific NO_x emissions changes (Fig. 9). For the LC B10, LC B20, and MC B20 fuels, the peak in-cylinder gas temperature was lower than the respective neat PDF value at low load (low average gas temperature) due to the cetane effect and higher at high load (high average gas temperature). The HC B10 and B20 fuels had a higher peak in-cylinder gas temperature than the HC fuel, which correlates with the increased NO_x emissions. Therefore, it was hypothesized that thermal NO_x was the cause of differences in NO_x created by the addition of biodiesel.

7 FUEL PROPERTY CORRELATIONS

To further the understanding of the NO_x and PM formation due to the biodiesel, the correlation between the change in the brake-specific NO_x emissions and the change in fuel properties between the biodiesel blends and their respective neat fuels from the transient and steady-state testing were examined. Table 2 shows each fuel property for which a correlation coefficient was derived for the FTP and each mode of the steady-state test. The steady-state brake-specific PM from the TEOM was

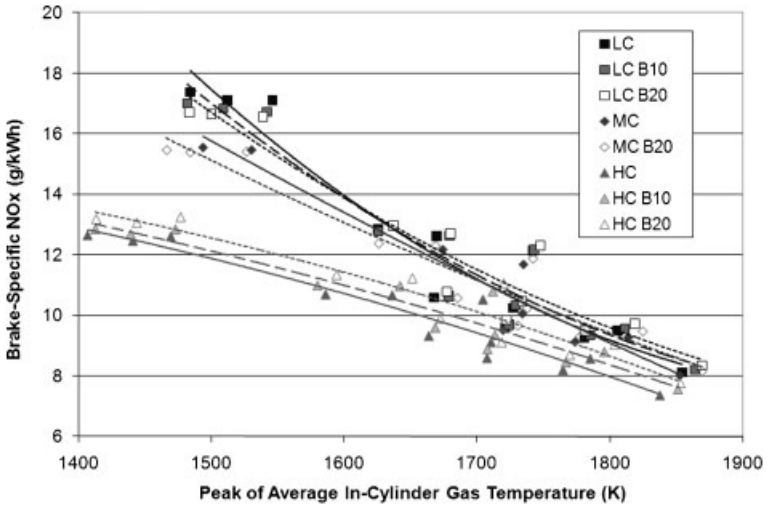

Fig. 9 Brake-specific NO_x correlated to the peak of the average in-cylinder gas temperature from the steady-state modes (solid lines, base fuels; dashed lines, B10 fuels; dotted lines, B20 fuels)

used as a surrogate for the gravimetric filter measurement. The correlation coefficient is a measure of the linear relationship between two variables and ranges from −1 to 1, with '−1' being a negative linear relationship, '+1' being a positive linear relationship, and zero having no linear relationship.

For the change in brake-specific PM with the biodiesel content, the highest correlations were for the change in the fatty acid methyl ester (FAME) content (by volume), fuel viscosity, percentage of oxygen in the fuel (by weight), oxygen-to-carbon ratio, and LHV (Fig. 10(a)). The FAME, fuel viscosity, percentage of oxygen in the fuel (by weight), and oxygen-to-carbon ratio were inversely related to the brake-specific PM emissions. As the LHV increased, the brake-specific PM increased. These fuel properties were inter-correlated except the fuel viscosity, which had low correlations with these four fuel properties. The correlation of PM emissions with oxygen content and the oxygen-to-carbon ratio has been shown in previous studies [**39**, **40**]. Cheng and colleagues [**40**] used numerical modelling to show that as the oxygen content increases, oxidation of carbon to CO and CO_2 increased in the premixed flame region, which reduces the carbon available for soot precursors. In addition, the increased oxygen

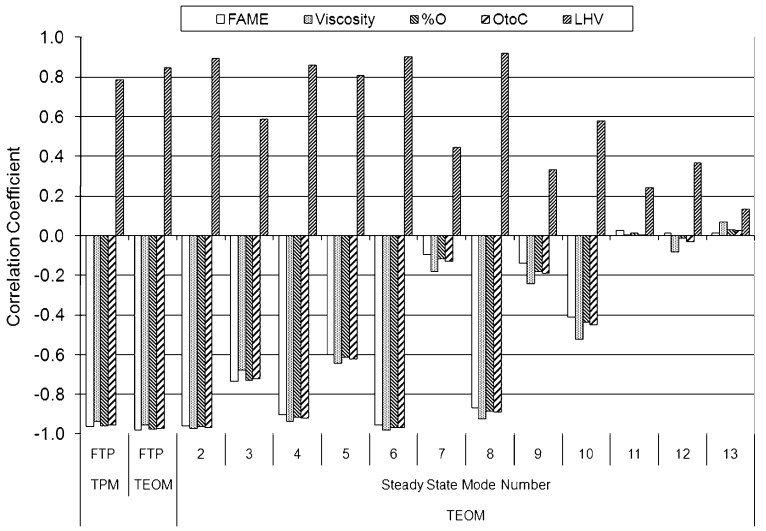

(a)

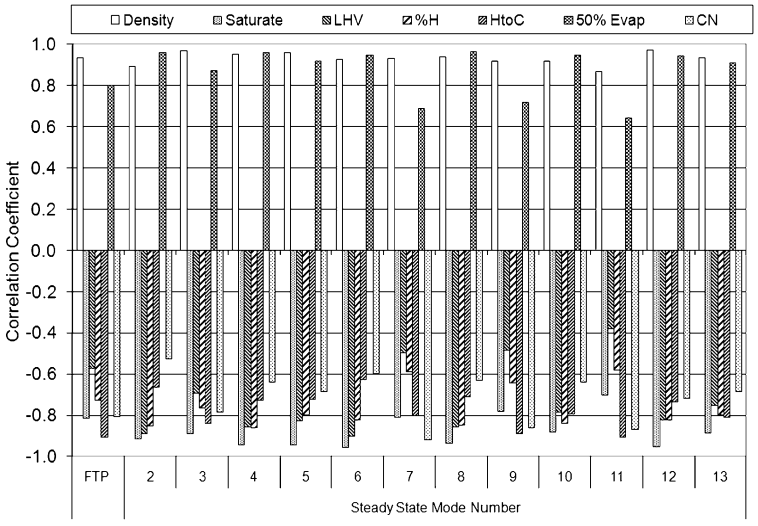

(b)

Fig. 10 The highest correlation coefficients between the change in brake-specific emissions and the change in fuel properties for the biodiesel blends with respect to their neat fuels: (a) PM; (b) NO_x

content increases radical content in the post premix flame region, which oxidize aromatics and limit the growth of polyaromatic hydrocarbons.

The highest correlations with change in brake-specific NO_x occurred with the change in fuel density, percentage of saturates in the fuel (by volume), LHV, percentage of hydrogen in the fuel (by weight), hydrogen-to-carbon ratio, the 50 per cent (by volume) boiling point temperature (BPT), and the cetane number (CN) (Fig. 10(b)). Note that these fuel properties were inter-correlated. As the fuel density and the 50 per cent distillation temperature increased with the biodiesel blends, NO_x increased. As percentage of saturates in the fuel, percentage of hydrogen in the fuel (by weight), hydrogen-to-carbon ratio, and the LHV increased with the biodiesel blends, NO_x decreased. As the level of hydrogen content in the fuel is increased, the saturated hydrocarbons should increase in addition to lowering the fuel density and increasing the LHV. Ban-Weiss and colleagues [**41**] attributed the slight NO_x increase with biodiesel to the higher degree of unsaturated hydrocarbons in biodiesel. Unsaturated hydrocarbons, which have more double bonds, were shown to have a higher adiabatic flame temperature than similar saturated hydrocarbons. The hydrogen-to-carbon ratio gives an indication of the degree of saturation for the fuel, with a low hydrogen-to-carbon ratio indicating a high number of double bonds. The B100, LC, MC, and HC fuels had a hydrogen-to-carbon ratio of 1.83, 1.73, 1.79, and 2.00, respectively. The correlation between the hydrogen-to-carbon ratio and the NO_x emissions was lower than the correlation between the percentage of saturates in the fuel and the NO_x emissions due to the B10 and B20 blends increasing in hydrogen-to-carbon ratio with the LC and MC fuels but decreasing with the HC fuel, and yet the NO_x emissions tended to increase for all B10 and B20 fuels. The correlation between the hydrogen-to-carbon ratio and NO_x emissions has been shown by previous researchers [**7**, **41**, **42**], but this correlation did not hold in this study.

The neat PDFs, B10, and B20 blends followed the trend of decreasing saturated hydrocarbons having increased NO_x (Fig. 11). At low loads (25–50 per cent loads), the trend is weaker because of the cetane effect. The change in cetane number had a high correlation with the change in brake-specific NO_x at 25 per cent load (Fig. 10(b), modes 7, 9, and 11). The influence of the degree of saturated hydrocarbons on NO_x was apparent for the neat PDFs and biodiesel blends, which followed the same trend line. Although the hydrogen-to-carbon ratio did not show a strong correlation, the percentage of saturates showed a strong correlation with the increase in NO_x emissions due to the different hydrocarbon compositions between diesel and soy biodiesel fuel. Any aromatics in the diesel fuel will have a high degree of unsaturation with a hydrogen-to-carbon ratio range of $\sim$0.7–1.7, while the unsaturated hydrocarbon components in soy biodiesel have a hydrogen-to-carbon ratio of $\sim$1.7–1.9. The saturated hydrocarbon components have a hydrogen-to-carbon ratio of $\sim$2.0–2.2 and $\sim$2.0 for diesel fuel and soy biodiesel, respectively. The diesel fuels had a high percentage of saturated hydrocarbons (50–90 per cent), but any aromatics in the diesel fuels impacted the overall number of double bonds, while the soy biodiesel had a low percentage of saturated hydrocarbons (13 per

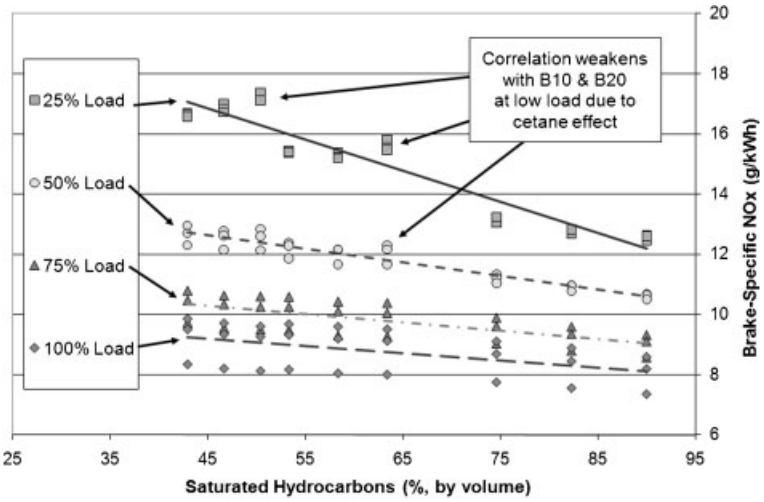

Fig. 11 Steady-state correlation between the brake-specific NO_x and the degree of saturated hydrocarbons at each mode (dashed lines are a linear trends line for 25, 50, 75, and 100 per cent load)

cent). A decrease in the adiabatic flame temperature as the percentage of saturated hydrocarbons increased, although the overall number of double bonds did not correlate well, would explain the reduction of the brake-specific NO_x emissions from the fuels tested.

The NO_x–PM trade-off is indicative of the combustion temperature effect, where higher combustion temperatures lead to lower PM and higher NO_x and vice versa. From the steady-state testing, the high loads (50–100 per cent load) followed the NO_x–PM trade-off (Fig. 12) and at low load (25 per cent load) there was a high degree of scatter. Part of the scatter at the low loads may be attributed to experimental error, where the dilution tunnel and analysers were optimized for the high power modes. The B10 and B20 blends followed the NO_x–PM curve of the neat fuel. A greater change in emissions occurred for the PM than the NO_x with the addition of biodiesel, which is expected. The change in PM with increasing biodiesel concentration may be due to both an oxygen content and the above defined combustion temperature effect (due to increased flame temperature), with the change in NO_x with increasing biodiesel concentration being due to the combustion temperature effect. It should be noted that the high data scatter at 25 per cent load was attributed to inaccuracy in the TEOM PM measurement (with one mode showing negative PM) due to adsorption and desorption of water vapour [**43**].

Another promising theory for the increase in NO_x emissions with biodiesel was suggested by Cheng and colleagues [**11**]; the decrease in soot with biodiesel lowers the radiation heat transfer, which causes increased local flame temperatures. The increase in NO_x emissions with biodiesel fuel was shown here to be caused by thermal NO_x from the increase in the peak of the average in-cylinder gas temperature and the PM–NO_x trade-off. If a reduction in soot increases local flame temperatures, then any oxygenate additive should behave similar to biodiesel blends since the oxygen in the fuel lowers the soot, which should, in turn, increase local flame temperatures and NO_x. Previous studies show varied results on NO_x emissions (some increase, some decrease) with an oxygenated fuel blended with diesel fuel [**19**, **20**, **44**]. Song *et al.* [**20**] was the only study to match the combustion phasing between the oxygenated blends and the base diesel fuel, which resulted in an increase in the NO_x emissions and decrease in the soot; similar to biodiesel blends. The oxygenated fuels that were blended with the diesel fuel had high hydrogen-to-carbon ratios (2.0–2.5 compared with 1.8 for diesel) and were saturated hydrocarbons, which would increase the percentage of saturated hydrocarbons for the blended fuel. If biodiesel blends are considered an oxygenate additive, then the correlation with the percentage of hydrocarbons does not hold.

8 CONCLUSIONS

Three different neat PDFs were admixed with 10 per cent and with 20 per cent (by volume) soy-derived biodiesel and tested on a heavy-duty diesel engine during transient and steady-state testing. The three neat PDFs incorporated in the test programme included a low, medium, and high cetane value. In-cylinder pressure was collected for the steady-

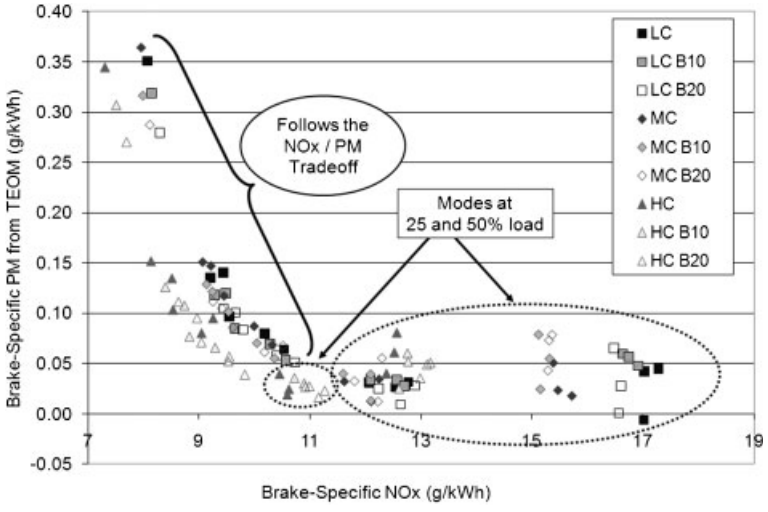

Fig. 12 NO_x–PM trade-off from the steady-state modes (excluding idle)

state and transient tests. The heat release and fuel properties were compared to the emissions of NO_x and PM with the following findings.

1. For the B10 fuels, the FTP integrated brake-specific FC, CO, THC, and TPM increased by 1–2 per cent, decreased by 5–6 per cent, decreased by 6–11 per cent (but the HC fuel was not statistically significant), and decreased by 10 per cent, respectively, compared with their neat PDFs. A statistically significant increase of 2–3 per cent, decrease of 7–12 per cent, decrease of 10–18 per cent, and decrease of 19–20 per cent was seen for the FTP integrated brake-specific FC, CO, THC, and TPM, respectively, for the B20 fuels compared with their neat PDFs.
2. During the transient testing, the integrated brake-specific NO_x emissions for the HC B10 and B20 fuels were statistically different from those of the HC fuel. The HC B10 fuel increased NO_x by 3 per cent and the HC B20 fuel increased NO_x by 5 per cent. The LC and MC B10 and B20 fuels emissions were not significantly different from their respective neat PDF emission values.
3. From the instantaneous NO_x mass emissions during the transient testing, the HC B10 and B20 fuels were shown to increase NO_x at all engine brake powers compared with the HC fuel and the LC and MC B10 and B20 fuels decreased NO_x at low power and increased NO_x at high power conditions compared with their respective neat PDFs.
4. The premix spike was reduced with increasing biodiesel content with the LC and MC fuels. A reduced ignition delay had more influence at low load than high load due to the high premix fraction at low load. The HC B10 and B20 fuels showed little change in the heat release curve and ignition delay with respect to the HC fuel.
5. The high cetane number of the biodiesel created a cetane or combustion phasing effect with the LC and MC B10 and B20 fuels. This 'cetane effect' shows the importance of matching cetane numbers between the neat petroleum diesel and biodiesel fuels. This 'cetane effect' is suspected to be the cause of varying results in the literature between studies on NO_x emissions with biodiesel blends compared with a neat PDF.
6. The brake-specific NO_x emissions from steady-state testing were related to the peak in-cylinder gas temperature. The LC and MC B10 and B20 fuels showed a lower peak in-cylinder gas temperature than their respective neat PDFs at low load and higher peak in-cylinder gas temperature at high load. Therefore, it is the authors' belief that the effect of biodiesel on NO_x emissions was based on thermal NO_x.
7. The reduction in PM emissions with increasing biodiesel content was found to correlate with the increase in oxygen content or the oxygen-to-carbon ratio.
8. High correlations between changes in the NO_x emissions and changes in the fuel properties (between the biodiesel blend and the neat fuel) were found with the change in fuel density, percentage of saturates in the fuel (by volume), percentage of hydrogen in the fuel (by weight), hydrogen-to-carbon ratio, the 50 per cent BPT, and the LHV. The cetane number did show a high correlation with NO_x emissions at 25 per cent load.
9. The biodiesel blends had a brake-specific NO_x–PM trade-off, suggesting a thermal NO_x effect. The biodiesel blends followed their respective neat fuel NO_x–PM trade-off suggesting the neat PDF properties limit the minimum obtainable NO_x emissions for biodiesel blends.
10. The high correlation at 75–100 per cent load between the unsaturated hydrocarbons and the brake-specific NO_x suggests that an increase in the unsaturated hydrocarbons (such as caused by adding biodiesel to the fuel) may increase the adiabatic flame temperature which would increase NO_x.
11. When adding biodiesel to diesel fuel, PM and NO_x emissions behaved similarly to a previous study [**20**] conducted with oxygenated fuel blends. Oxygenates have been shown to increase NO_x while increasing the percentage of saturates in the fuel, which would discredit the adiabatic flame temperature theory above and leave the theory that the decrease in radiation heat transfer creates increased local flame temperatures.

ACKNOWLEDGEMENTS

The authors acknowledge the dedication of Byron Rapp and Bradley Ralston of the West Virginia University Center for Alternative Fuels, Engines, and Emissions in supporting the acquisition of data included in this study.

REFERENCES

1 **Pope III, C.** Air pollution and health – good news and bad. *N. Engl. J. Med.*, 2004, **351**, 1132–1134.
2 **Maitre, A., Bonneterre, V., Huillard, L., Sabatier, P.,** and **de Gaudemaris, R.** Impact of urban

atmospheric pollution on coronary disease. *Eur. Heart J.*, 2006, **27**, 2275–2284.

3 **Code of Federal Regulations.** *CFR Title 40 Part 86–89*, 2004 (Office of the Federal Register National Archives and Records Administration, Washington, DC).

4 **Kowalewicz, A.** and **Wojtyniak, M.** Alternative fuels and their application to combustion engines. *Proc. IMechE, Part D: J. Automobile Engineering*, 2005, **219**, 103–125. DOI: 10.1243/095440705X6399.

5 **Wu, Y., Wang, M., Sharer, P.,** and **Rousseau, A.** Well-to-wheels results of energy use, greenhouse gas emissions and criteria air pollutant emissions of selected vehicle/fuel systems. SAE paper 2006-01-0377, 2006.

6 **Canakci, M.** Performance and emissions characteristics of biodiesel from soybean oil. *Proc. IMechE, Part D: J. Automobile Engineering*, 2005, **219**, 915–922. DOI: 10.1243/095440705X28736.

7 **McCormick, R., Alleman, T., Graboski, M., Herring, A.,** and **Tyson, K.** Impact of biodiesel source structure material and chemical structure on emissions of criteria pollutants from a heavy-duty engine. *Environ. Sci. Technol.*, 2001, **35**, 1742–1747.

8 **McCormick, R., Alvarez, J., Graboski, M., Tyson, K.,** and **Vertin, K.** Fuel additive and blending approaches to reducing NO_x emissions from biodiesel. SAE paper 2002-01-1658, 2002.

9 **McCormick, R., Alvarez, J.,** and **Graboski, M.**, NO_x solutions for biodiesel: final report, report no. NREL/SR-510-31465, US Department of Energy National Renewable Energy Laboratory, Golden, Colorado, 2003.

10 **McCormick, R.** Regulated emissions from biodiesel tested in heavy-duty engines meeting 2004 emission standards. SAE paper 2005-01-2200, 2005.

11 **Cheng, A., Upatnieks, A.,** and **Mueller, C.** Investigation of the impact of biodiesel fuelling on NO_x emissions using an optical direct injection diesel engine. *Int. J. Engine Res.*, 2006, **7**, 297–318. DOI: 10.1243/14680874JER05005.

12 **Eckerle, W., Lyford-Pike, E., Stanton, D., LaPointe, L., Whitacre, S.,** and **Wall, J.** Effects of methyl ester biodiesel blends on NO_x emissions. SAE paper 2008-01-0078, 2008.

13 **Szybist, J., Kirby, S.,** and **Boehman, A.** NO_x emissions of alternative diesel fuels: a comparative analysis of biodiesel and FT diesel. *Energy Fuels*, 2005, **19**(4), 1484–1492.

14 **Nuszkowski, J., Thompson, G. J.,** and **Clark, N. N.** Heat release and emission characteristics of B20 biodiesel fuels during steady state and transient operation. SAE paper 2008-01-1377, 2008.

15 **Hess, H., Boehman, A., Tijm, P.,** and **Waller, F.** Experimental studies of the impact of CETANER on diesel combustion and emissions. SAE paper 2000-01-2886, 2000.

16 **Liotta, F.** and **Mantalvo, D.** The effect of oxygenated fuels on emissions from a modern heavy-duty diesel engine. SAE paper 932734, 1993.

17 **Ullman, T., Spreen, K.,** and **Mason, R.** Effects of cetane number, cetane improver, aromatics, and oxygenates on 1994 heavy duty diesel engine emissions. SAE paper 941020, 1994.

18 **Zannis, T., Hountalas, D.,** and **Kouremenos, D.** Experimental investigation to specify the effect of oxygenated additive content and type on DI diesel engine performance and emissions. SAE paper 2004-01-0097, 2004.

19 **Lu, X., Yang, J., Zhang, W.,** and **Huang, Z.** Improving combustion and emissions of direct injection compression and emissions of direct injection compression ignition engines using oxygenated fuel additives combined with a cetane improver. *Energy Fuels*, 2005, **19**(5), 1879–1888.

20 **Song, J., Zello, V., Boehman, A.,** and **Waller, F.** Comparison of the impact of intake oxygen enrichment and fuel oxygenation on diesel combustion and emissions. *Energy Fuels*, 2004, **18**(5), 1282–1290.

21 **Thompson, G., Gibble, J., Clark, N.,** and **Gautam, M.** Influences of real-world conditions on in-use emission from heavy-duty diesel engines. SAE paper 2006-01-3393, 2006.

22 **Heywood, J. B.** *Internal combustion engine fundamentals*, 1988 (McGraw-Hill, New York, New York).

23 **Woshni, G.** A universally applicable equation for the instantaneous heat transfer coefficient in the internal combustion engine. SAE paper 670931, 1967.

24 **Brunt, M.** and **Platts, K.** Calculation of heat release in direct injection diesel engines. SAE paper 1999-01-0187, 1999.

25 **Yamane, K., Ueta, A.,** and **Shimamoto, Y.** Influence of physical and chemical properties of biodiesel fuels on injection, combustion and exhaust emission characteristics in a direct injection compression ignition engine. *Int. J. Engine Res.*, 2001, **2**, 249–261. DOI: 10.1243/1468087011545460.

26 **Schumacher, L., Chellappa, A., Wetherell, W.,** and **Russell, M.** *The physical & chemical characterization of biodiesel low sulfur diesel fuel blends*, 1995 (National Biodiesel Board, Jefferson City, Missouri).

27 **Podsiadlik, D., Chase, R., Lewis, D.,** and **Spears, M.** Phase-based TEOM measurements compared with traditional filters for diesel PM. SAE paper 2003-01-0783, 2003.

28 **Xu, S.** Comparison of heavy-duty truck diesel particulate matter measurement: TEOM and traditional filter. SAE paper 2005-01-2153, 2005.

29 **Brunt, M.** and **Pond, C.** Evaluation of techniques for absolute cylinder pressure correction. SAE paper 970036, 1997.

30 **Brunt, M.** and **Emtage, A.** Evaluation of burn rate routines and analysis errors. SAE paper 970037, 1997.

31 **Zhang, Y.** and **Boehman, A.** Impact of biodiesel on NO_x emissions in a common rail direct injection diesel engine. *Energy Fuels*, 2007, **21**(4), 2003–2012.

32 **Miyamoto, N., Chikahisa, T., Murayama, T.,** and **Sawyer, R.** Description and analysis of diesel

engine rate of combustion and performance using Weibe's functions. SAE paper 850107, 1985.
33 **Alkidas, A.** On the premixed combustion in a direct injection diesel engine. *J. Engng Gas Turbines Power*, 1987, **109**, 187–192.
34 **Nuszkowski, J.** *The effects of fuel additives on diesel engine emissions during steady state and transient operation*. Dissertation, West Virginia University, Morgantown, West Virginia, 2008.
35 **Dec, J.** A conceptual model of DI diesel combustion based on laser-sheet imaging. SAE paper 970873, 1997.
36 **Dec, J.** and **Canaan, R.** PLIF imaging of NO formation in a DI diesel engine. SAE paper 980147, 1998.
37 **Aceves, S., Flowers, D., Martinez-Frias, J., Smith, J., Dibble, R., Au, M.,** and **Girard, J.** HCCI combustion: analysis and experiments. SAE paper 2001-01-2077, 2001.
38 **Clark, N., Jarrett, R.,** and **Atkinson, C.** Field measurements of particulate matter emissions, carbon monoxide, and exhaust opacity from heavy-duty diesel vehicles. *J. Air Waste Mgmt Assoc.*, 1999, **49**, 76–84.
39 **Hallgren, B.** and **Heywood, J.** Effects of oxygenated fuels on DI diesel combustion and emissions. SAE paper 2001-01-0648, 2001.
40 **Cheng, A., Dibble, R.,** and **Buchholz, B.** The effect of oxygenates on diesel engine particulate matter. SAE paper 2001-01-1705, 2001.
41 **Ban-Weiss, G., Chen, J., Buchholz, B.,** and **Dibble, R.** A numerical investigation into the anomalous slight NO_x increase when burning biodiesel; a new (old) theory. *Fuel Process. Technol.*, 2007, **88**, 659–667.
42 **Schonborn, A., Ladommatos, N., Allan, R., Williams, J.,** and **Rogerson, J.** Effect of the molecular structure of individual fatty acid alcohol esters (biodiesel) on the formation of NO_x and particulate matter in the diesel combustion process. SAE paper 2008-01-1578, 2008.
43 **Jarrett, R.** and **Clark, N.** Evaluation of methods for determining continuous particulate matter from transient testing of heavy-duty diesel engines. SAE paper 2001-01-3575, 2001.
44 **Litzinger, T., Stoner, M., Hess, H.,** and **Boehman, A.** Effects of oxygenated blending compounds on emissions from a turbo-charged direct injection diesel engine. *Int. J. Engine Res.*, 2000, **1**, 57–70. DOI: 10.1243/1468087001545263.